

EX VIVO TERAHERTZ IMAGING REFLECTION OF MALIGNANT AND BENIGN HUMAN BREAST TUMORS

Amel Al-Ibadi*

Abstract: This study evaluated the effectiveness of spectroscopy and imaging tools, using a previously-unexplored (0.2- 1.4) terahertz range, for investigating tumors in human tissue and distinguishing between malignant and benign cancer cells. One advantage of this technique is that terahertz radiation in this frequency range passes through human tissue without causing ionization or any negative effects. To assess the effectiveness of this band of frequencies, THz data were collected from 10 different fresh breast tissue samples, extracted directly after excision. The optical properties were investigated at a range of low frequencies and THz imaging revealed good contrast between the different types of fresh tissue. Observations indicated that the optical and electrical properties in the low-frequency (0.3-0.5) range provided accurate information about breast cancer tissue. These results demonstrated the effectiveness of the technique up to 0.5 THz for ex vivo studies in medical applications.

Keywords: Terahertz imaging, terahertz radiation, medical & biological tissues and tissue characterizations.

1. Introduction

This Terahertz spectroscopy and imaging technique was used to produce two- or three-dimensional images of an object, using THz radiation (0.1 to 10THz) beamed directly or reflected through the samples, thus providing highly accurate information about tissues inaccessible to other technologies (Gong et al., 2020). Terahertz radiation is non-ionized (Peter et al., 2013) and harmless to the objects tested (Yu et al., 2012). Terahertz radiation, in the low-millimeter waveband, is highly absorbed in the water in living tissues (Wilmsink & Grundt, 2011). The Terahertz team used a terahertz technique to visualize and analyze human tissue, with the aim of detecting and identifying different types of cancer tumors and comparing these images with the results of laboratory analysis by a medical oncology team. Previous studies asserted that terahertz imaging facilitated early cancer detection in tissues, before it became visible, widespread, or sensitive to any other technique. Moreover, in samples exposed to terahertz radiation, diseased tissues were readily distinguished from healthy tissues, making this technique an effective tool for future medical applications (Cassar et al., 2018). In particular, the absorption and refraction coefficients of tumor tissues were higher than those of healthy tissues (Wahaia et al., 2020). Differences between tissue regions had previously been studied between 500 and 600 GHz (Al-Ibadi et al., 2017). The distinction, variation, and differences in physical characteristics between tissues are due to the presence of

water and changes in the composition of the infected tissue, such as higher cell and protein density and increased water content (Sun et al., 2013). Access to all information relating to the tissue is through exposure to terahertz radiation within a specified range of frequencies and the formation of adequate images of areas with confirmed or suspected tumors that distinguish them from healthy regions (Cassar et al., 2018). Previous research confirmed that cancer tumors had higher absorption and refraction factors than healthy tissues within a given frequency range (Fan et al., 2014). Terahertz spectroscopy is highly effective at distinguishing tumors from healthy tissues (El-Shenawee et al., 2019), thus helping surgeons remove tumors more precisely and avoid cutting out too much healthy tissue. The assurance of leaving no cancerous tissue in the patient's body minimizes the need for extensive removal of healthy tissue around the tumor, which is considered a safety precaution, but is prejudicial to patients and significantly extends recovery time, as well as avoiding repeated operations in the future. Recent research and studies suggest that the terahertz imaging technique is capable of distinguishing between infected and healthy tissue and provides valuable tissue-related diagnostic information that cannot be obtained using currently-available imaging techniques (Al-Ibadi et al., 2017).

Cancer is the second leading cause of death in the world, with outcomes exacerbated by late onset of symptoms and widespread lack of diagnostic and therapeutic services. Cells in malignant tumors (cancer) grow and divide rapidly and uncontrollably, leading to invasion and damage of natural

Authors information:

Biomedical physics department, College of medicine, University of Al-Qadisiyah, Iraq.

*Corresponding Author: MI_absq@yahoo.com

Received: January 22, 2022

Accepted: April 22, 2022

Published: September 30, 2022

tissue (WHO, 2017). The main diagnostic steps of examining tissue from the patient, identifying infected cells, distinguishing them from healthy tissue, and delivering the result may take at least 10 days. The diagnosis may be inaccurate, potentially leading to repeated excisions of infected tissue surrounded by insufficient amounts of intact tissue, which has not only physical, but also psychological and financial implications for the patient.

Cancer is not defined by one type or specific, persistent symptoms, since cancer cells continue unlimited division, accompanied by changes in their synthesis, functional and behavioral characteristics (Wang et al., 2014). Terahertz rays used to detect cancer and determine the degree of proliferation penetrate the tissue without causing any biological changes (Hejmadi, 2010).

The aim of this study on breast cancer was to identify the different regions in excised biological tissue and examine their physical properties, especially their dielectric properties, using terahertz imaging and spectroscopy to discriminate between tumors and normal tissue. THz radiation is produced by centering ultrafast (100fs) laser light on the space between the electrodes at near infrared wavelengths (a Ti:Sapphire laser with a central wavelength of 800 nm). Free-carrier acceleration results in the figuration of the transverse photoreceptor connected with an antenna, producing a wide band of frequencies between 100 GHz and 3 THz. Coherent photoconductor detection is achieved using a photonic antenna similar to the emitter. The signal-to-noise ratio is around 4000: 1, limited by the thermal noise of the antenna.

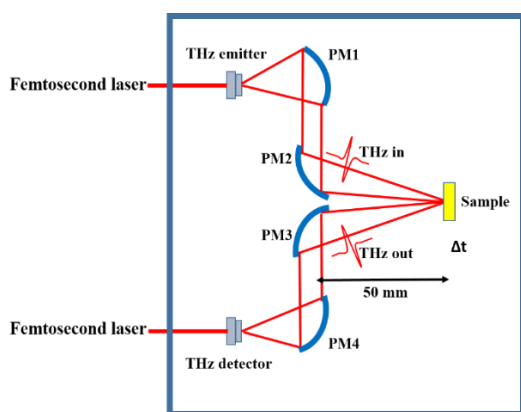


Figure 1. Schematic of Teraview system

2. Experimental Method

These experiments were conducted using a commercially-available TeraView 3000 (Teraview Ltd, Cambridge, UK, 2001) with a reflection system (Figure.1) to determine the complex dielectric properties of fresh tissues, initially to qualify the setup and data processing. A set of 10 fresh tissue samples were surgically removed from women's

breasts (age range: 40-60 years) for cancer analysis. The standard operating procedure was followed at the Bergonié Institute in Bordeaux (France) to obtain human tissue sections containing breast cancer. The sapphire substrate was chosen to avoid bio-impact. The sample was fixed on the motor to scan THz pulse reflectivity. Step size and acquisition time depended on sample size. The system was purged of water particles by injecting dry air. Spatial resolution was determined by our system setup and the frequency used in this work. The samples were fixed between two 1 mm-thick quartz plates with slight pressure to avoid air gaps between the tissue and the quartz surface (Figure 2). The reflected THz pulse was measured with and without the sample to extract data on the frequency-dependent physical properties of the sample, detected by the second reflected pulse (from the sapphire-sample interface). The optical properties of these samples in the 0.2-1.4 THz range are presented in Figure 4. THz spectroscopy was also used in reflective mode, focusing on the acquisition of images to determine breast cancer. Analysis of processed THz images in the time and frequency domain presented in Figure 3 and their optical properties were used to distinguish between tumors and healthy tissues with high accuracy. These THz images were highly correlated with the histopathological images.

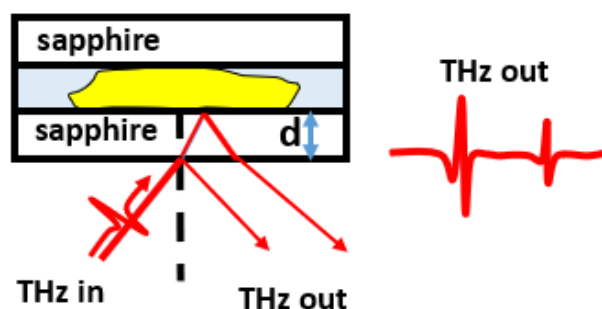


Figure 2. Schematic of the study sample (yellow) between two sapphire (white) windows with thickness (d). The two main reflex peaks. The bottom peak (THz out) reflected from the sapphire-air interface (without sample) and from the sapphire-sample interface (with sample).

2.1 Breast tissue sample preparation

After surgery, the tissues were prepared in accordance with standard laboratory methods for tissue collection, preparation, and fixation, for examination by pathologists at the Bergonié institute in Bordeaux (France). All samples were taken during breast surgery and all studies were histologically confirmed by a pathologist. Additionally, a pathologist identified diseased and healthy tissue in all samples for THz imaging. Appropriate healthy and infected tissues were determined by comparison with samples examined using the terahertz technique.

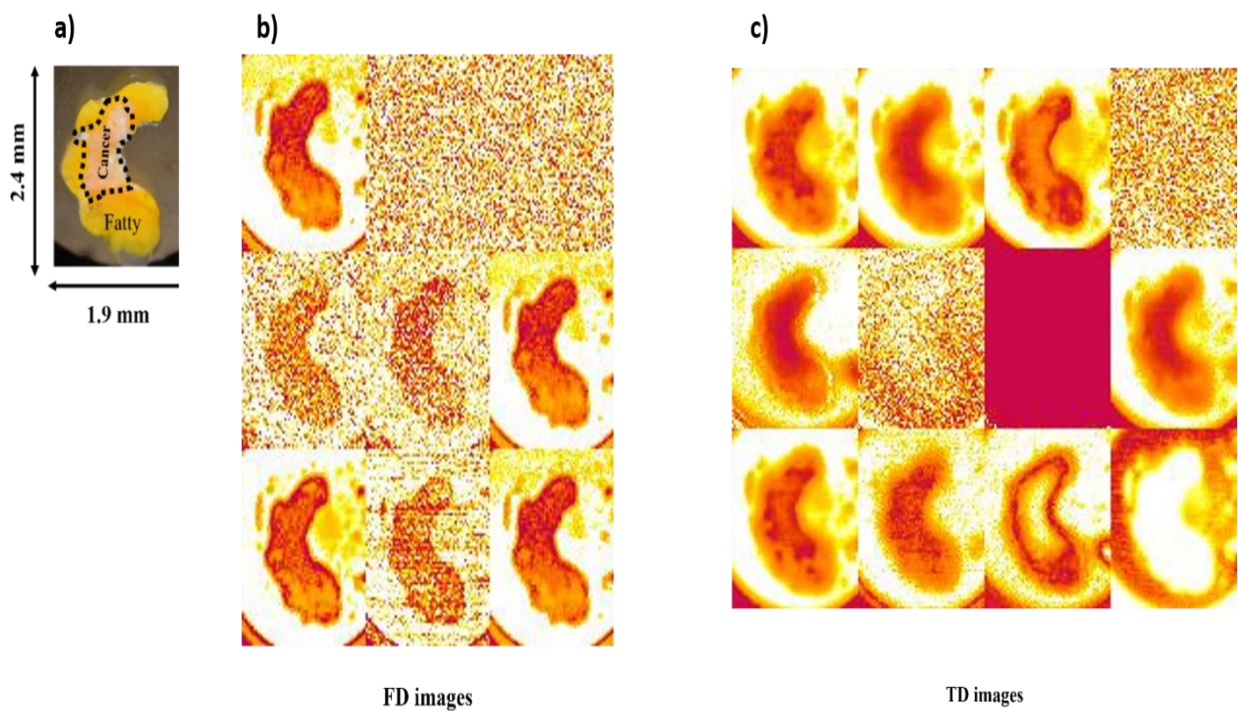


Figure 3. a) Optical image of the tissue studied, b and c) Automatic extraction of the different THz images based on the time-frequency domain, in order of mathematical operations, respectively, from left to right: Diff, Div, derivative, energy-entropy, FWHM [0-max] down, FWHM [0-max] up, FWHM [min-max] up, max, mean, min, mult, entropy-Shannon, and sum operation processes.

2.2 Data acquisition

The THz pulses were focused on a 3 mm-thick sample placed flat between the sapphire substrates at an incident angle of 10 deg. THz images were measured by a raster reflection scanning system, where the sample stage was moved two-dimensionally (2D) in an x-y plane on exposure to the THz waves with step size 0.2 mm, to measure the THz signals reflected in each pixel area. All reflection signals from the recorded samples scanned produced 4096 data points, giving a three-dimensional THz image. A two-dimensional image of the amplified signal through the THz scanning beam was created in each pixel of the image (Figure 4).

2.3 Image processing

After THz collection and processing, the data on the relevant frequency range was sufficiently accurate for feature detection. A number of challenges potentially accounted for error in our measurements, such as variations in biological tissue, including less-homogenous composition, uneven surfaces, changes through measurements, and aging. In the THz system, the curvature of the imaging window, irregular connection with the sample, and multiple reflections of THz pulses were also potential sources of error. For these reasons, mathematical operations, such as peak intensity and peak to peak intensity, were selected to obtain THz images based on the time-frequency domain (Ballacey et

al., 2016). Processing thus determined the intensity level of each pixel in the image, to ensure that the THz images would provide accurate data on the amplitude of the THz signal reflected from the fresh tissue in various positions, over a range of frequencies, as shown in Figure 4a.

2.4 Data processing

Data processing was applied to the THz images and the optical properties of the samples. This involved removing background noise by averaging each pixel signal. These signals were then isolated from the dataset, using a zero-padding algorithm to improve the second peak interface of the remaining signal (Fan et al., 2016). The information related to the application of the time domain in the fast Fourier transform process (FFT) was converted to the frequency domain. Analytical data were processed using MATLAB code.

3. Results

Different THz images of the 0.2 mm-thick fresh tissue samples on a sapphire window, recorded at 0.8 THz in reflection mode, were obtained by automatic processing, using mathematical operations in both time and frequency domains, and distinguished between cancerous (abnormal) and fatty (healthy) regions, see Figure 3. The imaging results

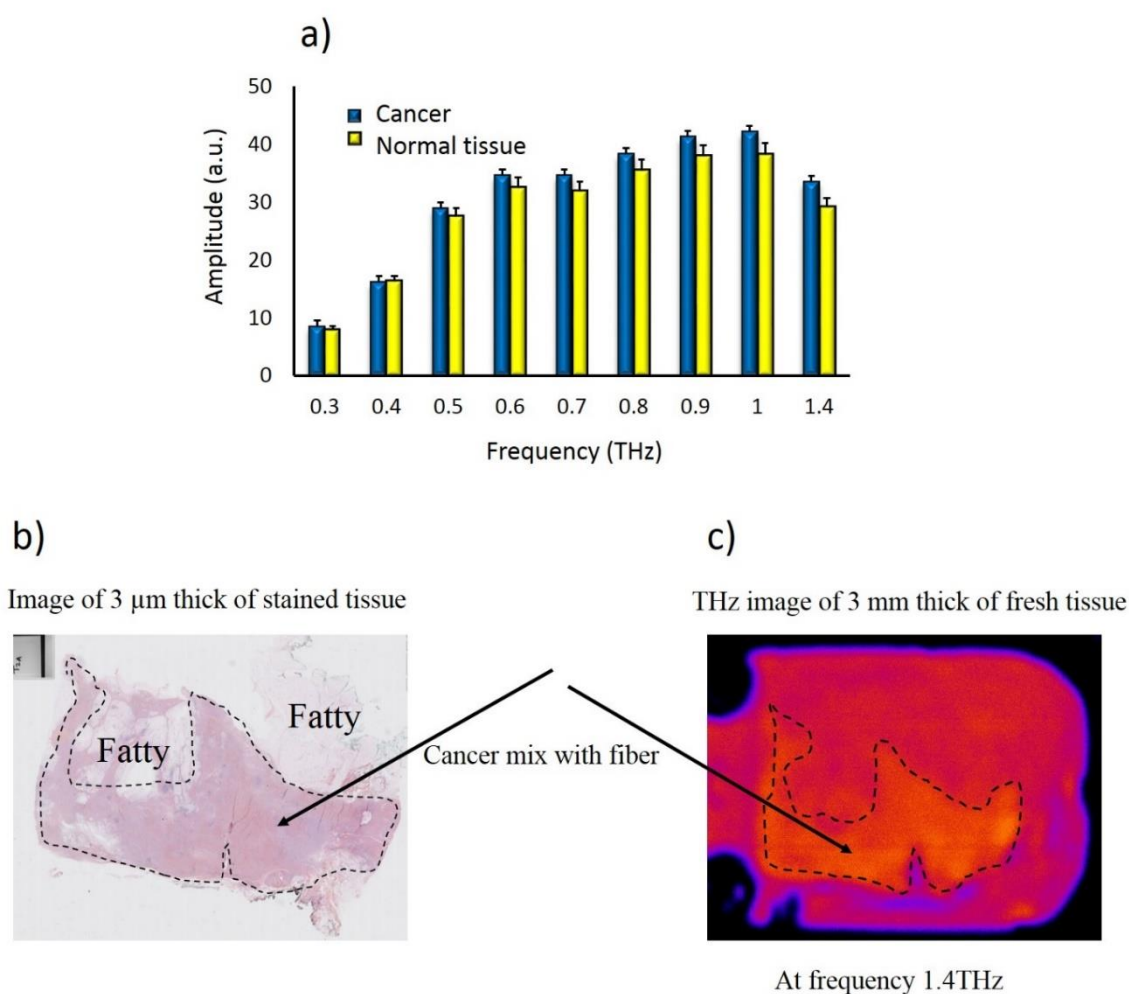


Figure 4. a) Absorption coefficients of infected (cancerous) and healthy tissue, b) Image of a 3 micrometer-thick stained tissue sample, c) image of a 3 millimeter-thick sample of the same tissue at a frequency of 1.4 THz.

varied depending on the different mathematical operations, but this method provided rapid identification of cancer tissues compared with standard clinical reports. Tumors were clearly delineated in the THz images in the frequency and time domain, compared with histopathology images, showing the distribution of cancer cells within the fatty regions. Additionally, good agreement was observed between fatty and cancer tissue in both techniques. The variation in image contrast in the time-frequency domain may be explained by differences in biological composition between fat and cancer tissues.

Figure 4 (b & c) shows the close match between the 1.4 THz image and that of the 3 μm-thick tissue sample embedded in a paraffin block, where the infected region shows more variation than the healthy region. In terms of physical analysis, the results confirmed that identification of the cancer region was more effective than the healthy region, as shown in Figure 4a, comparing the average amplitude of tumors and normal tissue. Significant differences in amplitude were clearly observed at frequencies ranging from 0.2 to 1.4 THz. Figure 4a illustrates

the behavior of THz pulses progressing through each region of fresh breast tissue.

The average values for tumors and healthy tissues at 1 THz were $44.6 \text{ (a.u.)} \pm 0.23$ and 40.3 ± 0.20 , respectively. Thus, the fatty tissue exhibited less frequency-dependent amplitude, which may explain the increased THz reflection pulses on the THz detector, while the cancer tissue exhibited higher amplitude. In addition, Figure 4a shows that amplitudes for the normal and cancer tissues decreased at 1.4 THz, possibly suggesting that the THz signals reflected from the sample fell to the noise floor. Different regions of the sample are clearly distinguished and there was good correspondence between the THz images and histopathology slides.

The THz data was processed to extract refractive indices, absorption coefficients and averages of biological tissues from different regions, as reported in Table 1. The results revealed that, in the 0.3- 0.5 THz range, the optical properties (refractive indices and absorption coefficients) of normal tissue were lower than those of abnormal tissue (cancer). In addition, the dielectric properties of normal and

Table 1. Parameters of water by the Double Debye model and measured data in the 0.3 to over 0.5 THz range. (RI, α , σ and ϵ) are the refractive index, absorption coefficient, conductivity, and permittivity of water and human tissue, respectively.

Material	0.3 THz				0.4 THz				0.5 THz			
	RI	α	σ	ϵ	RI	α	σ	ϵ	RI	α	σ	ϵ
Water-Debye model	2.7	103	4.3	6.5	2.6	118	4	6.3	2.5	136	3.2	6
Water from our measurements	2.9	129	5.8	8.6	2.7	149	5	7.7	2.6	170	4.2	6.9
Abnormal tissue	2.6±4.9%	99±5%	4.9	7.3	2.5±4.8%	107±5.4%	3.3	6.7	2.4±4.7%	128±6%	3	6.1
Normal tissue	2.4±1.7%	75±1.2%	3	6.3	2.3±1.6%	91±1.5%	2.7	5.8	2.2±1.5%	109±3.3%	2.4	5.4

abnormal tissues were calculated using a Debye double-relaxation model (Pashkin et al., 2003). Furthermore, a water reference was measured before the tissue samples were processed to correct variations in data extraction using Equation 1. A detailed description of the extraction of the refractive index and absorption coefficient is given in the article cited (Pashkin et al., 2003):

$$\epsilon_c = \epsilon_\infty + \frac{\epsilon_s - \epsilon_1}{1 + i\omega\tau_1} + \frac{\epsilon_1 - \epsilon_\infty}{1 + i\omega\tau_2} \quad (1)$$

Where ϵ_c is the dielectric function, ϵ_∞ is the dielectric constant at high frequencies, ϵ_s is the static dielectric constant, ϵ_1 is the dielectric function of the long and fast relaxation process, occurring over τ_1 and τ_2 , respectively, at pulsation ω . These results indicated that the dielectric properties (conductivity (σ) and permittivity (ϵ)) (Joyce et al., 2016) of normal tissue were lower than those of abnormal tissue. The refractive index $n(\omega)$ and absorption coefficient $\alpha(\omega)$ of the sample were calculated using the equation.

For data analysis, the frequency-dependent absorption coefficient and refractive index were obtained using equations 2 and 2, respectively, giving values of α_{sample} , and n_{sample} . A detailed description of the extraction of the refractive index and absorption coefficient is given in the article cited (Fan et al., 2016).

$$n_s = \text{real}(\tilde{n}_s(\omega)) \quad (2)$$

$$\alpha_s = \frac{2\omega \cdot k(\omega)}{c} \quad (3)$$

These results showed that the optical properties of fresh tissue, especially the refractive index (RI) and absorption coefficients (α), measured ex- vivo by spectral analysis in the 0.3-0.5 THz range, were systematically higher in tumors than in healthy tissue. In addition, the measured complex dielectric properties of the tissues increased, so we

compared the conductivity and permittivity of abnormal and normal tissue with those of water. Consequently, the interaction of THz radiation with fresh tissue provided valuable information for quantifying the dielectric properties of breast tissue in the THz range. Moreover, the measured dielectric properties of the different breast tissues differed from the extracted data, depending on their optical properties. The significant difference between normal breast and cancerous tissue revealed that analysis of THz reflection parameters had the potential to differentiate between tumors and healthy tissues. Details of these THz properties are presented with average values and standard errors in Table 1. In conclusion, THz reflection spectroscopy is capable of measuring the dielectric coefficients of tumor and healthy tissue, and differentiating between them, due to their different structures. In addition, the identification of cancerous and healthy tissue in each sample was verified by a histopathologist, who provided information on the tissue types for evaluating the accuracy of the reflected THz spectroscopy measurements.

5. Conclusions

A comparison of terahertz radiation imaging with classic, slide-based tissue samples confirmed that this technique has the potential to provide reliable detection of cancer tumors. The accuracy of the THz technique varied among the different types of complex excised breast tissues and substrate materials used in this study, possibly due to scattering effects or the interaction of THz radiation with samples and substrates, as shown in Figure 3.

6. References

Al-Ibadi, A., Cassar, Q., Zimmer, T., MacGrogan, G., Mavarani, L., Hillger, P., Grzyb, J., Pfeiffer, U. R., Guillet, J. P., & Mounaix, P. (2017). THz spectroscopy and imaging for breast cancer detection in the 300-500 GHz range.

- International Conference on Infrared, Millimeter, and Terahertz Waves, IRMMW-THz, Spp 1857*, 1–1. <https://doi.org/10.1109/IRMMW-THz.2017.8067037>
- Ballacey, H., Al-Ibadi, A., MacGrogan, G., Guillet, J. P., Macpherson, E., & Mounaix, P. (2016). Automated data and image processing for biomedical sample analysis. *International Conference on Infrared, Millimeter, and Terahertz Waves, IRMMW-THz, 2016-Novem*, 2–3. <https://doi.org/10.1109/IRMMW-THz.2016.7758882>
- Cassar, Q., Al-Ibadi, A., Mavarani, L., Hillger, P., Grzyb, J., MacGrogan, G., Zimmer, T., Pfeiffer, U. R., Guillet, J.-P., & Mounaix, P. (2018). Pilot study of freshly excised breast tissue response in the 300 – 600 GHz range. *Biomedical Optics Express*, 9(7), 2930. <https://doi.org/10.1364/boe.9.002930>
- El-Shenawee, M., Vohra, N., Bowman, T., & Bailey, K. (2019). Cancer detection in excised breast tumors using terahertz imaging and spectroscopy. *Biomedical Spectroscopy and Imaging*, 8(1–2), 1–9. <https://doi.org/10.3233/bsi-190187>
- Fan, S., He, Y., Ung, B. S., & Pickwell-Macpherson, E. (2014). The growth of biomedical terahertz research. *Journal of Physics D: Applied Physics*, 47(37). <https://doi.org/10.1088/0022-3727/47/37/374009>
- Fan, S., Parrott, E. P. J., Ung, B. S. Y., & Pickwell-MacPherson, E. (2016). Calibration method to improve the accuracy of THz imaging and spectroscopy in reflection geometry. *Photonics Research*, 4(3), A29. <https://doi.org/10.1364/prj.4.000a29>
- Gong, A., Qiu, Y., Chen, X., Zhao, Z., Xia, L., & Shao, Y. (2020). Biomedical applications of terahertz technology. *Applied Spectroscopy Reviews*, 55(5), 418–438. <https://doi.org/10.1080/05704928.2019.1670202>
- Hejmadi, M. (2010). Introduction to Cancer Biology. In *Expert Opinion on Pharmacotherapy* (2nd editio, Vol. 2, Issue 4). <https://doi.org/10.1517/14656566.2.4.613>
- Joyce, H. J., Boland, J. L., Davies, C. L., Baig, S. A., & Johnston, M. B. (2016). A review of the electrical properties of semiconductor nanowires: Insights gained from terahertz conductivity spectroscopy. *Semiconductor Science and Technology*, 31(10). <https://doi.org/10.1088/0268-1242/31/10/103003>
- Pashkin, A., Kempa, M., Němec, H., Kadlec, F., & Kužel, P. (2003). Phase-sensitive time-domain terahertz reflection spectroscopy. *Review of Scientific Instruments*, 74(11), 4711–4717. <https://doi.org/10.1063/1.1614878>
- Peter, B. S., Yngvesson, S., Siqueira, P., Kelly, P., Khan, A., Glick, S., & Karellas, A. (2013). Development and testing of a single frequency terahertz imaging system for breast cancer detection. *IEEE Transactions on Terahertz Science and Technology*, 3(4), 374–386. <https://doi.org/10.1109/TTHZ.2013.2241429>
- Sun, K., Tordjman, J., Clément, K., & Scherer, P. E. (2013). Fibrosis and adipose tissue dysfunction. *Cell Metabolism*, 18(4), 470–477. <https://doi.org/10.1016/j.cmet.2013.06.016>
- Wahaia, F., Kašalynas, I., Minkevičius, L., Carvalho Silva, C. D., Urbanowicz, A., & Valušis, G. (2020). Terahertz spectroscopy and imaging for gastric cancer diagnosis. *Journal of Spectral Imaging*, 9, 1–8. <https://doi.org/10.1255/jsi.2020.a2>
- Wang, Y., Chen, D., Qian, H., Tsai, Y. S., Shao, S., Liu, Q., Dominguez, D., & Wang, Z. (2014). The Splicing Factor RBM4 Controls Apoptosis, Proliferation, and Migration to Suppress Tumor Progression. *Cancer Cell*, 26(3), 374–389. <https://doi.org/10.1016/j.ccr.2014.07.010>
- WHO. (2017). Guide to Cancer - Guide to cancer early diagnosis. In *World Health Organization*. <https://apps.who.int/iris/bitstream/handle/10665/254500/9789241511940-eng.pdf;jsessionid=2646A3E30075DB0FCA4A703A481A5494?sequence=1>
- Wilmink, G. J., & Grundt, J. E. (2011). Invited Review Article : Current State of Research on Biological Effects of Terahertz Radiation. *J Infrared Milli Terahz Waves*, 32, 1074–1122. <https://doi.org/10.1007/s10762-011-9794-5>
- Yu, C., Fan, S., Sun, Y., & Pickwell-Macpherson, E. (2012). The potential of terahertz imaging for cancer diagnosis: A review of investigations to date. *Quantitative Imaging in Medicine and Surgery*, 2(1), 33–45. <https://doi.org/10.3978/j.issn.2223-4292.2012.01.04>